

RESEARCH ARTICLE

Molecular compartmentalization in a syncytium: restricted mobility of proteins within the sea urchin skeletogenic mesenchyme

Jian Ming Khor*, Jennifer Guerrero-Santoro and Charles A. Ettensohn[‡]

ABSTRACT

Multinucleated cells, or syncytia, are found in diverse taxa. Their biological function is often associated with the compartmentalization of biochemical or cellular activities within the syncytium. How such compartments are generated and maintained is poorly understood. The sea urchin embryonic skeleton is secreted by a syncytium, and local patterns of skeletal growth are associated with distinct subdomains of gene expression within the syncytium. For such molecular compartments to be maintained and to control local patterns of skeletal growth: (1) the mobility of TFs must be restricted to produce stable differences in the transcriptional states of nuclei within the syncytium; and (2) the mobility of biomineralization proteins must also be restricted to produce regional differences in skeletal growth. To test these predictions, we expressed fluorescently tagged forms of transcription factors and biomineralization proteins in sub-domains of the skeletogenic syncytium. We found that both classes of proteins have restricted mobility within the syncytium and identified motifs that limit their mobility. Our findings have general implications for understanding the functional and molecular compartmentalization of syncytia.

KEY WORDS: Echinoderm, Sea urchin, Skeletogenesis, Primary mesenchyme, Syncytium, Gene regulatory network

INTRODUCTION

Multinucleated cells, also known as syncytia, are found across the tree of life (Ogle et al., 2005; Mela et al., 2020; Olsen, 2020; McCartney and Dudin, 2023). Syncytia can arise in two ways: through nuclear division in the absence of cytokinesis or through cell-cell fusion. In multicellular animals, syncytia first appear during embryonic development. Some embryonic syncytia, such as the cleavage-stage syncytial embryos of many arthropods and the syncytiotrophoblast of placental mammals, are transient (Carvalho and Heisenberg, 2010; Stathopoulos and Newcomb, 2020; Renaud and Jeyarajah, 2022), whereas others, such as myotubes, persist into adulthood (Kim et al., 2015). Syncytia arise in adult animals during the normal process of cell differentiation, e.g. when macrophages fuse to produce osteoclasts (Kloc et al., 2022). Syncytia can also arise under pathogenic conditions, when host cell fusion is triggered by viral and bacterial pathogens (Leroy et al., 2020; Lin et al., 2021; Bzdyl et al., 2022). In some well-studied cases, biochemical and

Department of Biological Sciences, Carnegie Mellon University, 4400 Fifth Avenue, Pittsburgh, PA 15218, USA.

D J.M.K., 0000-0002-1428-6770; C.A.E., 0000-0002-3625-0955

Handling Editor: Cassandra Extavour Received 23 March 2023; Accepted 23 October 2023 cellular activities, such as gene expression programs and patterns of nuclear division, are regionalized with syncytia (Bursztajn et al., 1989; Fogarty et al., 2011; Roberts and Gladfelter, 2015; Dundon et al., 2016; Gerber et al., 2022). Such studies reveal that distinct molecular and functional compartments can exist within a single, large, multinucleated cell. The mechanisms that underlie the generation and maintenance of such compartments, however, are poorly understood.

The development of the calcareous endoskeleton of the sea urchin embryo is a powerful model for the analysis of morphogenesis, cell differentiation, biomineralization and the evolution of development (Oliveri et al., 2008; Ettensohn, 2009, 2020; Koga et al., 2014; McIntyre et al., 2014; McClay, 2016; Shashikant et al., 2018a,b; Gildor et al., 2021; Ben-Tabou de Leon, 2022; Ettensohn et al., 2022). The embryonic skeleton is produced by primary mesenchyme cells (PMCs), a specialized population of biomineral-forming cells derived from the micromeres of the 16-cell stage embryo. PMCs undergo an epithelial-to-mesenchymal transition at the late blastula stage and migrate into the blastocoel cavity, where they adopt a characteristic ring-like pattern between the vegetal pole and the equator of the embryo. During this migratory phase, PMC filopodia fuse with one another, creating a slender cytoplasmic cable that connects the cells in a single, continuous, syncytial network. Amorphous calcium carbonate and associated proteins are secreted into a membrane-bound compartment within the cytoplasmic cable, and the biomineralized rods that comprise the embryonic skeleton are assembled within this compartment.

Skeletal patterning provides evidence of the regional specialization of the PMC syncytium. Overt skeletogenesis begins at the mid-gastrula stage, when two tri-radiate skeletal rudiments are deposited within the PMC syncytium at stereotypical positions along the ventrolateral aspects of the blastocoel wall. The three arms of each skeletal rudiment subsequently elongate and branch in a stereotypical manner, with each rudiment producing an elaborate half-skeleton that is the mirror image of its partner. The different rods of the skeleton elongate at characteristic rates, and although some cease growth during embryogenesis, others grow continuously (Guss and Ettensohn, 1997; Descoteaux et al., 2023). Local variations in skeletal growth provide strong evidence of functional compartmentalization within the PMC syncytium.

Skeletal growth and patterning is mediated by short-range signals provided by the adjacent ectoderm (Okazaki, 1975; Armstrong et al., 1993; Guss and Ettensohn, 1997). Several signaling molecules secreted by the ectoderm are responsible for this control. The best characterized of these signaling molecules is VEGF3, which plays an essential role in skeletal development throughout the echinoderm phylum (Duloquin et al., 2007; Fujita et al., 2010; Knapp et al., 2012; Morino et al., 2012; Adomako-Ankomah and Ettensohn, 2013, Adomako-Ankomah and Ettensohn, 2014; Ettensohn and Adomako-Ankomah, 2019; Morgulis et al., 2019; Morgulis et al.,

^{*}Present address: National Institutes of Health, Bethesda, MD 20892, USA.

[‡]Author for correspondence (ettensohn@cmu.edu)

2021). During early sea urchin embryogenesis, VEGF3 is produced by the ectoderm at the sites where the skeletal rudiments will form, and at later stages the protein is expressed by ectoderm cells at the growing tips of the skeletal rods that support the larval arms. VEGF3 interacts with a receptor tyrosine kinase, VEGFR-10-Ig, that is expressed specifically by PMCs (Duloquin et al., 2007). Two additional secreted proteins, FGF and TGFB, also regulate skeletogenesis, although these factors are less well characterized (Röttinger et al., 2008; Sun and Ettensohn, 2017; Adomako-Ankomah and Ettensohn, 2013, 2014). The ectodermal territories that express VEGF and FGF (and possibly TGFB, which has not been studied in this regard) are established through the coordinated activity of several signaling pathways, including the Nodal, BMP and Wnt pathways (Duboc et al., 2004; Flowers et al., 2004; Duloquin et al., 2007; Röttinger et al., 2008; Yaguchi et al., 2010; McIntyre et al., 2013).

PMC differentiation is controlled by a well-characterized gene regulatory network (GRN) (Oliveri et al., 2008; Shashikant et al., 2018a,b). One cardinal function of this network is to activate the expression of a large battery of PMC-specific proteins that mediate biomineralization, including proteins that regulate calcium uptake, proton transport, bicarbonate synthesis, phase transitions of calcium carbonate, and many other proteins that affect the mineral and/or protein components of the biomineral (reviewed by Ettensohn et al., 2022). The PMC GRN network is activated before gastrulation in a cell-autonomous fashion within the presumptive PMCs. Based on qualitative whole-mount in situ hybridization studies, the initial cell-autonomous phase of GRN deployment produces a homogeneous population of cells; i.e. effector genes are expressed uniformly among PMCs at the late blastula stage (Rafiq et al., 2012, 2014). During gastrulation, however, the regulation of the network shifts to a signal-dependent mode and region-specific patterns of gene expression arise within the PMC syncytium. Many mRNAs are expressed in specific sub-domains of the PMC syncytium at late stages, including mRNAs developmental that biomineralization proteins and transcription factors that positively regulate biomineralization genes (Harkey et al., 1992; Guss and Ettensohn, 1997; Illies et al., 2002; Livingston et al., 2006; Sun and Ettensohn, 2014). In general, regions of elevated mRNA expression correspond to regions of active skeletal growth (i.e. at the sites where the skeletal rudiments form and, at later developmental stages, at the tips of the arms). Based on these observations, it has been proposed that regional variations in skeletal growth and patterning during embryogenesis are a consequence of local, signaldependent modulation of the skeletogenic GRN (Harkey et al., 1992; Guss and Ettensohn, 1997; Sun and Ettensohn, 2014).

Because skeletogenesis occurs within a syncytium, if localized mRNAs are to produce local differences in skeletal growth, at least two conditions must be met. First, to maintain stable, local differences in the transcriptional states of individual PMC nuclei within the syncytial network, the mobility of TFs that regulate the expression of biomineralization genes must be restricted. Rapid diffusion of these proteins would prevent the formation of stable, distinct nuclear regulatory states within the syncytium. Second, even if local differences in transcriptional regulatory states are maintained, the mobility of downstream effector proteins that directly mediate biomineralization must also be restricted to produce local control of skeletal growth. Consistent with these hypotheses, some transcription factors and biomineralization proteins are concentrated in sub-domains of the PMC syncytium, as determined by immunostaining of fixed embryos (Urry et al., 2000; Gross et al., 2003; Luo and Su, 2012). In addition, Wilt et al. (2008) examined GFP-tagged forms of two spicule matrix proteins, Sp-SM30 and Sp-SM50, in transgenic embryos and noted that both showed non-uniform distributions.

In the present study, we directly tested both predictions by expressing fluorescently tagged forms of various PMC transcription factors and biomineralization proteins in sub-domains of the PMC syncytium and analyzing the mobility of the proteins in living embryos. Our findings show that both classes of proteins have restricted mobility, providing a mechanism for the establishment and maintenance of distinct molecular and functional compartments within the syncytium.

RESULTS

To examine the mobility of proteins within the PMC syncytium, we C-terminally tagged wild-type (full-length) and mutant forms of several transcription factors and biomineralization proteins with GFP or mCherry. To express proteins specifically in PMCs, we cloned their coding regions into plasmids and used a well-characterized, intronic *cis*-regulatory element (CRE) of the *S. purpuratus* gene *LOC115919257* (a gene previously referred to as WHL22.691495 or *Sp-EMI/TM*) to drive expression in transgenic embryos (Shashikant et al., 2018a,b; Khor et al., 2019). Below, we refer to this intronic regulatory element as the 'PMC CRE'. Although this CRE was originally derived from *S. purpuratus*, it is also active in *L. variegatus*, which is the species used in this study (Khor and Ettensohn, 2023). In both species, the *LOC115919257* CRE drives reporter gene expression only in PMCs, with expression first detectable at the mesenchyme blastula stage, before PMC fusion

In sea urchins, microinjection of plasmids into one-cell zygotes results in the mosaic incorporation and expression of transgenes (McMahon et al., 1985). Injection of a mixture of plasmids invariably results in co-expression of the constructs, presumably through assembly of the molecules into a mixed concatenate before integration (Arnone et al., 1997). In our studies, if plasmid DNA was incorporated into cells of the micromere lineage, this usually produced a genetically mosaic PMC syncytium. Typically, we coinjected a plasmid encoding a complementary fluorescent protein (i.e. GFP, in the case of mCherry-tagged fusion proteins, and mCherry, in the case of GFP-tagged fusion proteins). Many previous studies have shown that GFP and mCherry rapidly diffuse through the PMC syncytium (Arnone et al., 1997; Amore and Davidson, 2006; Wahl et al., 2009; Damle and Davidson, 2011; Shashikant et al., 2018a,b; Khor et al., 2019; Wang et al., 2019; Khor and Ettensohn, 2023). The primary reason for co-expressing GFP or mCherry was to confirm that a complete PMC syncytium had formed in each transgenic embryo that we scored, thereby demonstrating that any restricted distribution of tagged fusion proteins we observed was a consequence of limited protein mobility within the syncytium and not a failure of cell-cell fusion. In addition, expression of GFP or mCherry provided a direct comparison of the mobility of any tagged fusion protein with that of a highly diffusible reference protein in the same embryo. The distribution of fluorescently tagged proteins was analyzed in living embryos at post-gastrula stages (i.e. after the formation of the PMC syncytium) by epifluorescence and differential interference contrast (DIC) microscopy.

In initial studies, we used a single-plasmid expression system. The coding region of an mCherry-tagged protein of interest was cloned into a modified version of the widely used EpGFPII plasmid, with transcription of the fusion protein gene directly controlled by the PMC CRE in combination with the basal promoter of *Sp-endo16*

(Fig. 1). We refer to this as a 'constitutive' expression system (in contrast to an inducible system, described below), as the spatiotemporal pattern of expression of transgenes is determined solely by regulatory information intrinsic to the PMC CRE. Using this approach, we analyzed the mobility of five proteins within the PMC syncytium: three transcription factors (Sp-Alx1, Sp-Ets1 and Sp-Jun) and two biomineralization proteins (Sp-P16 and Sp-SM30B). All three transcription factors are normally expressed by PMCs during embryogenesis, and Sp-Alx1 and Sp-Ets1 provide positive regulatory inputs into many genes that have essential roles in skeletal development (Oliveri et al., 2008; Rafiq et al., 2014; Khor et al., 2019). P16 is a PMC-specific transmembrane protein required for skeletal growth (Cheers and Ettensohn, 2005), and SM30B is a major protein constituent of the spicule matrix (Wilt et al., 2013). It should be noted that, in these initial studies, proteincoding sequences were derived from the S. purpuratus genome (v.5.0) (Arshinoff et al., 2022), while microinjections were carried out using the more optically transparent eggs of L. variegatus. In subsequent experiments using the two-plasmid Tet-On system (below), protein sequences were obtained from a recently improved L. variegatus genome assembly (Davidson et al., 2020), and expression was again assessed in L. variegatus embryos. In three cases (Alx1, Jun and P16), we tested both S. purpuratus and L. variegatus forms of proteins. In all three cases, we detected no species-specific differences and found that all forms were highly localized within the PMC syncytium of L. variegatus, as described below.

Experiments using the constitutive expression system confirmed that in 100% of the embryos examined (n>200), GFP was distributed throughout the entire PMC syncytium at post-gastrula stages (Fig. 1Ba-c). GFP accumulated preferentially in PMC nuclei but was also detectable in the cytoplasm, including the PMC cytoplasmic cable. In contrast, four out of the five fusion proteins exhibited a restricted distribution within the PMC syncytium (Ets1 was a special case, as described below). For each of these constructs, >50% of transgenic embryos exhibited a highly restricted distribution of the fusion protein relative to the co-expressed reference GFP (n>30 in all cases) (Fig. 1Ba-d). Fluorescently tagged proteins were usually expressed in a single, continuous territory within the PMC syncytium, even though the PMC CRE first activates gene expression before PMC fusion. This finding is consistent with evidence that that PMCs do not disperse widely during migration and fusion, but instead tend to remain in the vicinity of their original site of ingression (Peterson and McClay, 2003). The size of the sub-domain of labeled PMCs varied from embryo to embryo, however, even within a single experimental trial. This reflected the random, mosaic incorporation and expression of transgenes in sea urchins, which result in variable numbers of PMC progenitors that expressed the constructs. Embryo-to-embryo differences in the level of expression based on position effects associated with the random insertion of the transgenes may also have contributed. We found that co-injection of two plasmids, each of which encoded a spatially localized protein (e.g. Sp-P16.WT.mCherry and a tagged histone, Sp-H2B.GFP) (Fig. 1Bf) resulted in identical localization of the two fusion proteins, confirming that co-injected plasmids are expressed by the same cells, as has been previously reported (Arnone et al., 1997).

The subcellular distributions of tagged fusion proteins varied. Transcription factors (Sp-Alx1.WT.mCherry and Sp-Jun.WT.mCherry) were highly concentrated in PMC nuclei (Fig. 1Bc,d; Fig. S1A). When a tagged form of Ets1 was expressed, however, we did not detect labeled nuclei within the PMC syncytium; instead, small

numbers of fluorescent cells were observed in the blastocoel, which is unassociated with the syncytium (data not shown). This suggested that overexpression of Ets1 under the control of the PMC CRE may have altered the specification of presumptive PMCs. With respect to biomineralization proteins, mCherry-tagged P16 (Sp-P16.WT.mCherry) was localized on the PMC surface, including PMC filopodia and the cytoplasmic cable, whereas SM30B (Sp-SM30B.WT.mCherry) was concentrated in puncta, primarily in cell bodies but also along the cytoplasmic cable (Fig. 1Be; Fig. S1A). Because P16 and SM30B, like many biomineralization proteins, are targeted to the secretory pathway, we asked whether the N-terminal signal sequence (SS) of P16 was required for its restricted distribution. Surprisingly, a fluorescently tagged form of P16 that lacked this sequence (Sp-P16ΔSS.GFP) exhibited a highly restricted distribution within the PMC syncytium that matched the distribution of co-expressed, wild-type P16 (Fig. 1Bd,e). The subcellular targeting of P16ΔSS.GFP, however, was distinct from that of the wild-type protein. P16ΔSS.GFP was not expressed on the PMC surface but was instead retained in the cytoplasm in a reticular pattern and was concentrated in the perinuclear region (Fig. 1Be). This apparent subcellular targeting of P16ΔSS.GFP, which is perhaps attributable to the transmembrane domain of the protein, may have limited its mobility within the PMC syncytium, even in the absence of the N-terminal signal sequence.

We extended these observations using a recently developed Tet-On system for inducing transgene expression in sea urchin embryos (Khor and Ettensohn, 2023). This system uses two plasmids: one that carries the reverse tetracycline-controlled transactivator (rtTA or TetOn3G) gene under the transcriptional control of the PMC CRE; and another that carries a gene encoding a fusion protein of interest under the control of Tet response elements. Transgene expression is rapidly induced when doxycycline (Dox) is added to the seawater. The inducible system offered several advantages over the constitutive system. First, induction of protein expression after the PMC syncytium had formed provided a more direct test of the mobility of proteins that are translated within the syncytium during late embryogenesis. Second, we found that the inducible system usually resulted in higher levels of expression of fluorescently tagged fusion proteins, which facilitated in vivo imaging. Third, we reasoned that by inducing the expression of transcription factors at late developmental stages, we might avoid any respecification of cells that resulted from overexpression of these proteins earlier in development, as appeared to occur after Ets1 overexpression.

Using this approach, we analyzed the mobility of six proteins within the PMC syncytium: three transcription factors (Lv-Alx1, Lv-Ets1 and Lv-Jun) and three biomineralization proteins (Lv-P16, Lv-SM29 and Lv-Clectin). S. purpuratus orthologues of four of these proteins were also examined using the constitutive expression system, as described above. The two additional proteins, Lv-SM29 and Ly-Clectin, are members of the spicule matrix protein family, which also includes SM30B (Livingston et al., 2006). Using the inducible system, wild-type or mutant forms of the proteins were tagged with GFP, and their distributions were compared with free mCherry or with other wild-type or mutant proteins tagged with mCherry. In all experiments, Dox was added at the prism stage, after PMC fusion was complete and the syncytium was well formed. Embryos were typically examined after 5-6 h of Dox exposure, at the early two-armed pluteus stage. For some constructs that were expressed at low levels, embryos were allowed to develop overnight in the presence of the drug and scored at the late two-armed pluteus

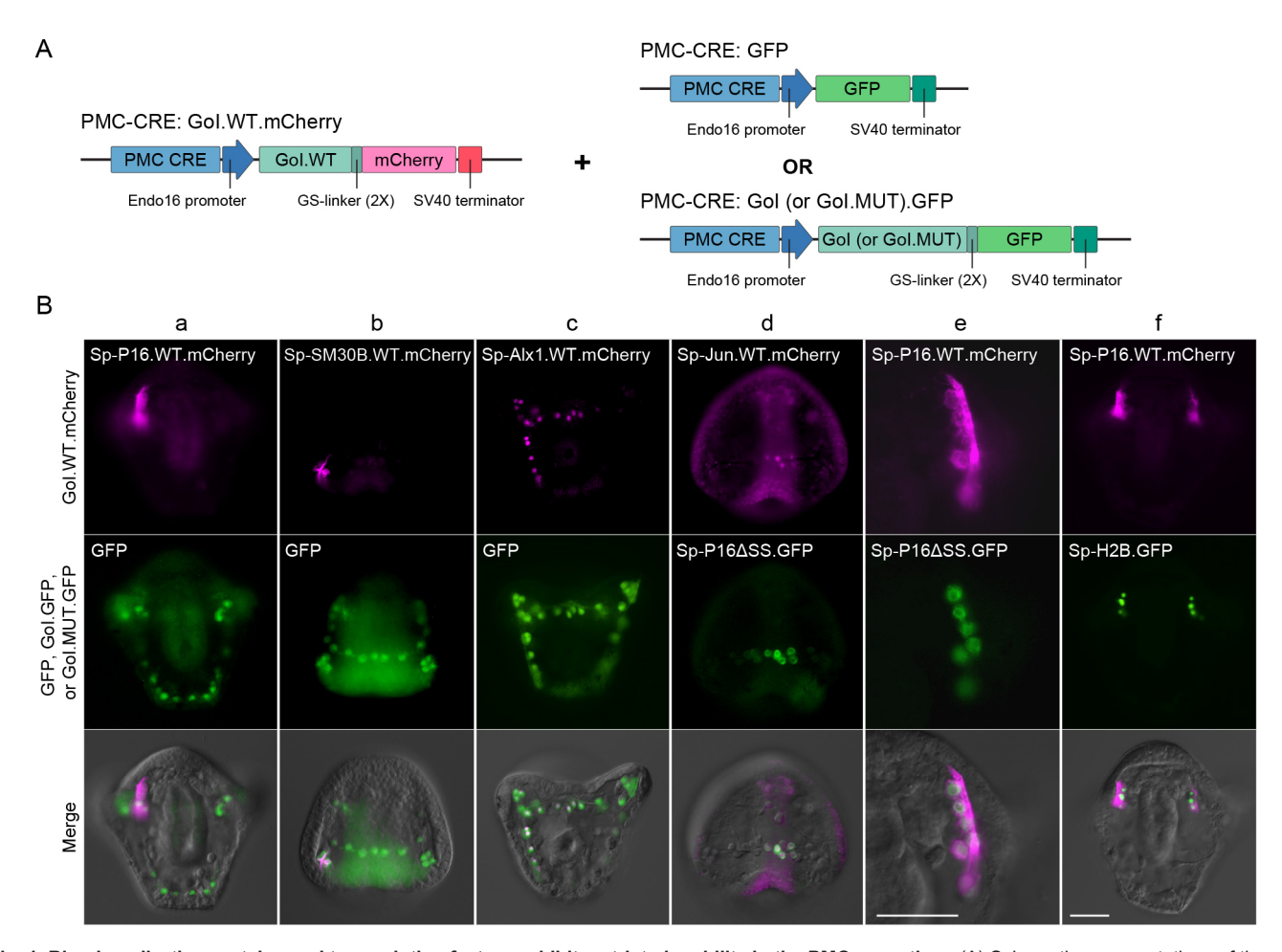


Fig. 1. Biomineralization proteins and transcription factors exhibit restricted mobility in the PMC syncytium. (A) Schematic representations of the expression constructs used to examine protein mobility. Plasmids were based on EpGFPII and the expression of each transgene was driven specifically in PMCs by an intronic CRE of the *S. purpuratus* gene *LOC115919257* (Shashikant et al., 2018a,b; Khor et al., 2019) ('PMC CRE' in the figure). Each line drawing represents a separate plasmid. (B) Representative images of live transgenic embryos. As GFP can readily diffuse throughout the PMC syncytium, the entire PMC network is labeled in transgenic embryos, despite the mosaic incorporation and expression of transgenes in sea urchins. (a-d) Wild-type proteins tagged with mCherry (Sp-P16.WT.mCherry, Sp-SM30B.WT.mCherry, Sp-Alx1.WT.mCherry and Sp-Jun.WT.mCherry) all showed localized distribution within the PMC syncytium. (e) Deletion of the endoplasmic reticulum signal sequence of Sp-P16 (Sp-P16ΔSS.GFP) did not enhance the mobility of the protein, although its subcellular distribution was altered. (f) Co-injection of two plasmids, each of which encoded a spatially localized protein (Sp-P16.WT.mCherry+Sp-H2B.GFP and Sp-Jun.WT.mCherry+Sp-P16ΔSS.GFP) always resulted in colocalization of the two fusion proteins, confirming that the two plasmids were expressed by the same cells. Top row: mCherry fluorescence. Middle row: GFP fluorescence. Bottom row: mCherry and GFP fluorescence overlaid onto differential interference contrast (DIC) images. (a,e,f) Abanal views of early pluteus larvae. (b,d) Lateral views of prism stage embryos. (c) Anal view of an early pluteus larva. Gol: gene of interest. Scale bars: 40 μm (bar in f applies to a-d,f; bar in e applies to e).

Studies using the inducible system were consistent with those based on constitutive expression and confirmed the restricted distributions of transcription factors and biomineralization proteins within the PMC syncytium. As expected, in 100% of the embryos examined (n>400), free reporter protein (GFP or mCherry) was distributed throughout the entire PMC syncytium, over a wide range of expression levels (Fig. 2Ba-f). In contrast, each of the six fusion proteins exhibited a restricted distribution within the PMC syncytium (Fig. 2a-f; Fig. S2A,B). The fraction of all embryos expressing a given transgene that exhibited a restricted domain of protein expression ranged from 61% to 91%, depending on the specific construct (n=33-58) (Table S2). Analysis of embryos in this class confirmed that, for each of the six proteins analyzed, the average number of PMC cell bodies with detectable levels of the tagged protein was significantly smaller (P<0.05) than the number of cell bodies that contained mCherry, which was co-expressed in the same embryos (Fig. 2C; Table S2). Taken together, these findings demonstrate the restricted mobility of the three

transcription factors and three biomineralization proteins we tested. As was the case when protein expression was controlled using the constitutive system, fusion proteins were usually localized in a single, continuous territory within the PMC syncytium, the size and location of which varied from embryo to embryo. The subcellular distributions of the tagged fusion proteins were also consistent with those observed in studies using the constitutive system. All three transcription factors (Lv-Alx1, Lv-Ets1 and Lv-Jun) were highly concentrated in PMC nuclei, while biomineralization proteins were localized on the PMC cell surface and along the spicules (Lv-P16) or in the cytoplasm and spicule compartment (Lv-SM29 and Lv-Clectin) (Fig. 2Ba-f; Fig. S1B).

Theoretically, the localization of tagged proteins in specific subdomains of the PMC syncytium could arise through long-distance protein translocation coupled with selective targeting to (or trapping at) specific sites. This mechanism seemed highly unlikely given that every protein we tested exhibited a restricted distribution, and each protein exhibited diverse patterns of localization across populations

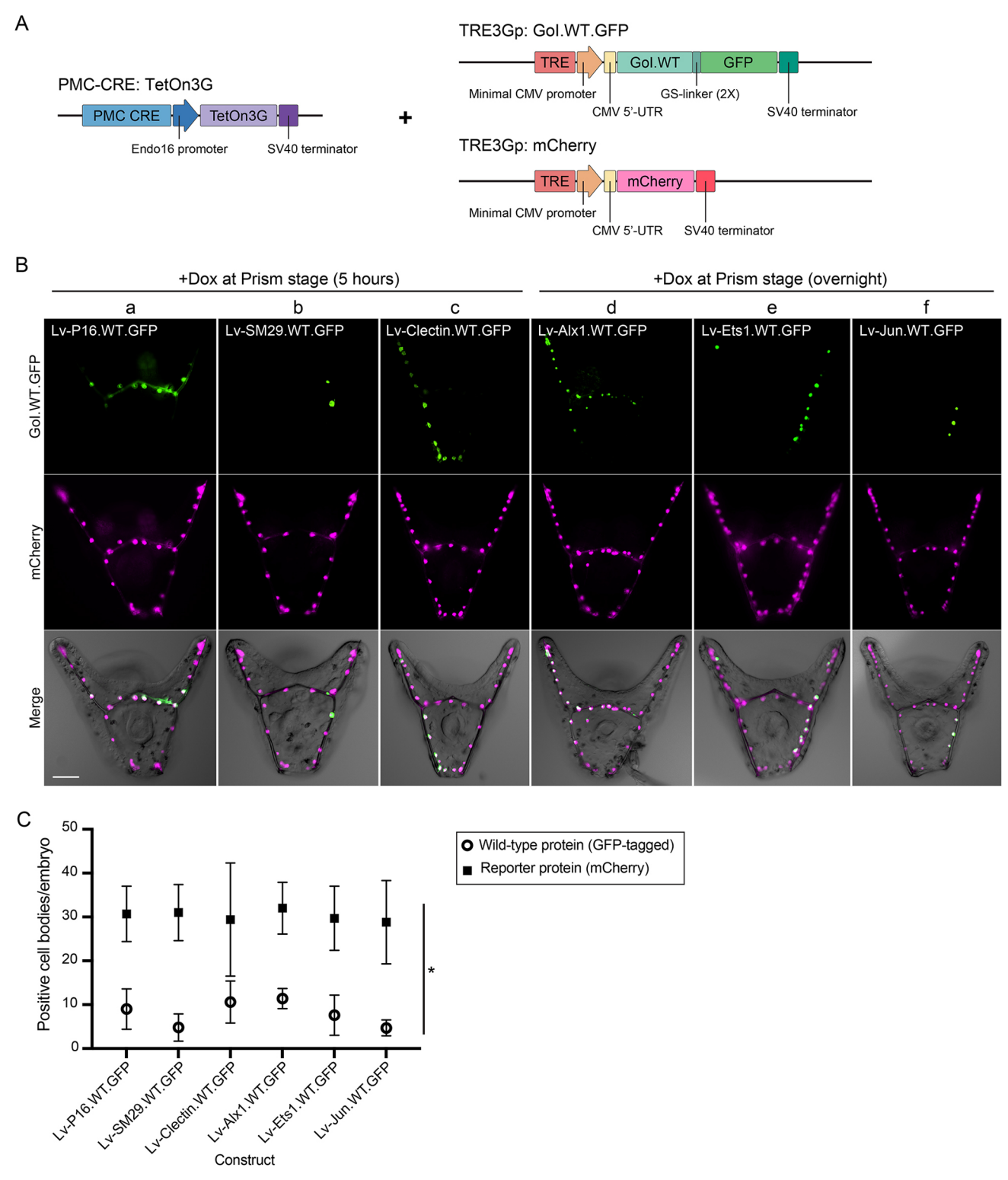


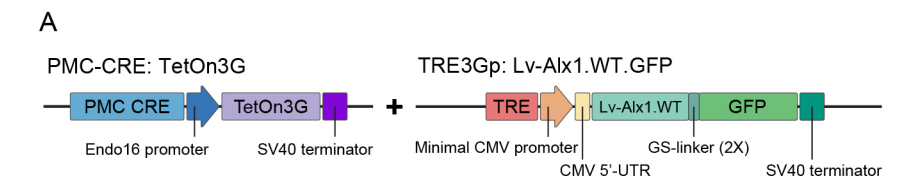
Fig. 2. Biomineralization proteins and transcription factors exhibit restricted mobility in the PMC syncytium. (A) Schematic representation of the Tet-On transactivator and responder constructs used to induce PMC-specific expression of GFP fusion proteins and wild-type mCherry. Each line drawing represents a separate plasmid. (B) Anal views of live transgenic pluteus larvae after Dox-induced gene expression. As mCherry protein can readily diffuse throughout the PMC syncytium, the entire PMC network is labeled in transgenic embryos, despite the mosaic incorporation and expression of transgenes in sea urchins. (a-c) GFP-tagged biomineralization proteins (Lv-P16.WT.GFP, Lv-SM29.WT.GFP and Lv-Clectin.WT.GFP) showed localized expression within the PMC syncytium. (d-f) GFP-linked transcription factors (Lv-Alx1.WT.GFP, Lv-Ets1.WT.GFP and Lv-Jun.WT.GFP) displayed strong nuclear localization in a subset of PMCs. Top row: GFP fluorescence. Middle row: mCherry fluorescence. Bottom row: GFP and mCherry fluorescence overlaid onto differential interference contrast (DIC) images. Gol: gene of interest. Scale bar: 50 μm. (C) Cell counts. Live embryos were imaged by conventional epifluorescence microscopy. For each embryo, one or two focal planes were collected; these were typically anal views that imaged PMC cell bodies along the postoral and body rods. The numbers of cell bodies within the PMC syncytium that contained the indicated tagged proteins or diffusible reference protein (mCherry) were counted. Data are mean±s.d. *P*-values were calculated using two-sample paired *t*-tests (**P*<0.05). See also Table S2.

of embryos. Nevertheless, to directly test whether proteins translocate over long distances or instead remain near the site of translation, we carried out combined immunofluorescence/RNA in situ hybridization on transgenic embryos that expressed Lv-Alx1.GFP. The distribution of Lv-alx1.GFP mRNA was assessed by in situ hybridization using a labeled probe complementary to the GFP-coding sequence, and the distribution of Lv-Alx1.GFP protein was examined in the same specimen using an affinity-purified antibody that recognizes GFP. These experiments revealed that reporter mRNA and protein were co-localized in the same region of the PMC syncytium (Fig. 3). Interestingly, in 100% of the embryos examined (13/13), the distribution of the Lv-Alx1.GFP protein was slightly broader than that of the mRNA, with the protein typically present in four or five additional cells/embryo that did not express detectable levels of mRNA. This difference between the number of mRNA-positive cells (mean=5.5, s.d.=2.5) and the number of protein-positive cells (mean=9.9, s.d.=3.8) was highly significant (P<0.0001, paired, two-tailed t-test), confirming that the Alx1 protein was more widely distributed than the mRNA, although the protein still exhibited highly restricted mobility within the syncytium. We conclude that the restricted distribution of Lv-Alx1.GFP, and presumably that of other proteins, is not due to longdistance targeting or trapping, but instead reflects the tendency of proteins to remain near the site of synthesis.

We next analyzed the roles of specific protein domains in restricting mobility within the PMC syncytium (see Fig. S3). Each transcription factor we examined contains a DNA-binding domain that also includes nuclear localization sequences (Boulukos et al.,

1989; Tagawa et al., 1995; Okamura et al., 2009; Khor and Ettensohn, 2017). Deletion of the complete DNA-binding domains (including the nuclear localization sequences) of Lv-Alx1, Lv-Ets1 and Lv-Jun dramatically increased the mobility of all three proteins within the syncytium relative to the corresponding, wild-type forms (Fig. 4Ba-c,C, Fig. S2C, Table S2). The mutant forms of these proteins were also less tightly restricted to the nucleus than the wildtype forms (Fig. 4Bd). Next, we tested whether the DNA binding domains of Alx1 and Ets1 were sufficient to restrict protein mobility when fused to fluorescent reporters. Through co-expression studies, we directly compared the mobility of reporter proteins fused to the complete DNA binding domains of each of the three transcription factors (Lv-Alx1.DBD.mCherry, Lv-Ets1.DBD.mCherry and Lv-Jun.DBD.mCherry) with the mobility of reporter proteins fused to DNA-binding domains that lacked flanking nuclear localization motifs (Lv-Alx1.DBDANLS.GFP, Lv-Ets1.DBDANLS.GFP and Lv-Jun.DBD\(Danger) (Fig. 5). The results of these studies depended on the specific construct. Fusions containing the DNAbinding domains (with or without flanking nuclear localization sequences) of Lv-Alx1 or Lv-Jun appeared to have little effect on the mobility of fluorescent reporters within the PMC syncytium and clearly did not restrict these proteins to a degree comparable to that of wild-type full-length Lv-Alx1 or Lv-Jun (compare Figs 2 and 5). Addition of the complete DNA-binding domain of Lv-Ets1, however, dramatically reduced the mobility of mCherry (Fig. 5Bb, Fig. 5C; Table S2).

Many proteins that mediate biomineralization are targeted to the spicule compartment via the secretory pathway (Livingston et al.,



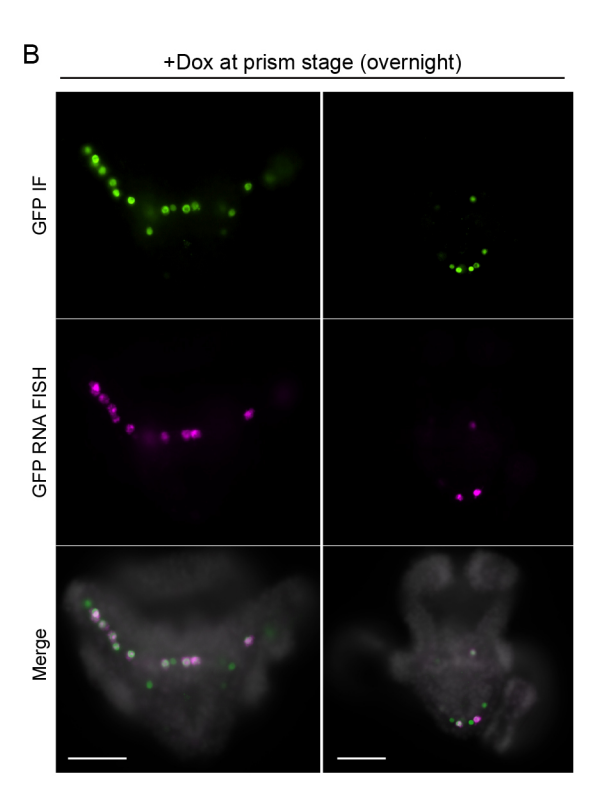


Fig. 3. The localization of proteins within the PMC syncytium in transgenic embryos is due to limited mobility and not to long-distance trafficking. (A) Schematic representation of the Tet-On transactivator and responder constructs used to induce PMC-specific expression of Lv-Alx1.WT.GFP. Each line drawing represents a separate plasmid. (B) GFP immunoFISH labeling of two fixed, transgenic embryos expressing Lv-Alx1.WT.GFP. In each embryo, Lv-Alx1.WT.GFP protein was localized to the same subdomain of the PMC syncytium as Lv-alx1.WT.GFP mRNA. In each case, the distribution of the GFP-tagged fusion protein was slightly broader than that of the cognate mRNA. Top row: GFPimmunostained cells. Middle row: Cy3-labeled gfp RNA transcripts. Bottom row: fluorescence merged with Hoechst 33342 counterstain (shown in grayscale). Scale

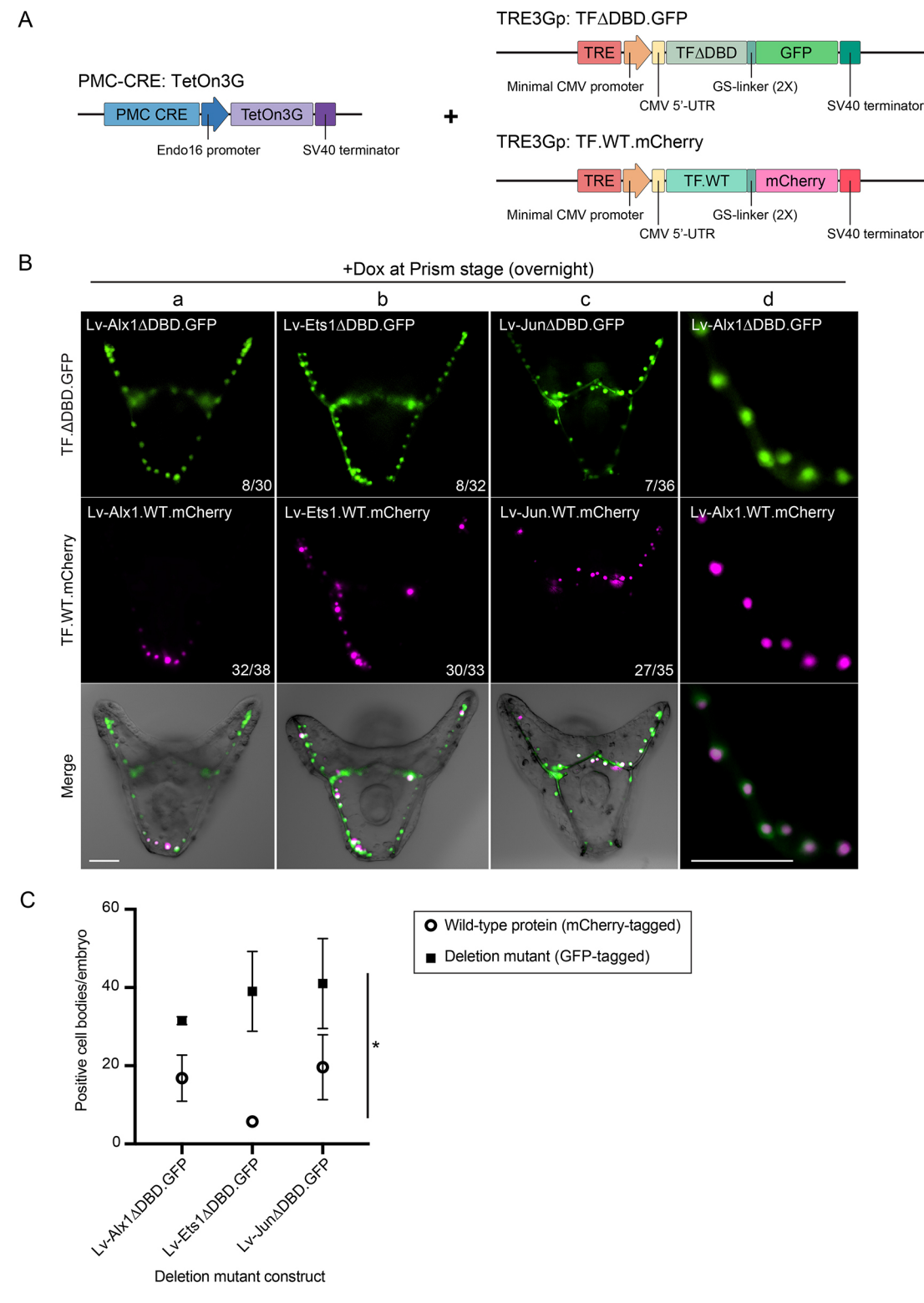


Fig. 4. Sea urchin transcription factors lacking DNA-binding domains readily diffuse throughout the PMC syncytium. (A) Schematic representation of the Tet-On transactivator and responder constructs used to induce PMC-specific expression of GFP and mCherry fusion proteins. Each line drawing represents a separate plasmid. (B) Anal views of live, transgenic pluteus larvae after Dox-induced gene expression. (a-c) GFP-linked transcription factors lacking DNA-binding domains (DBDs) (Lv-Alx1ΔDBD.GFP, Lv-Ets1ΔDBD.GFP and Lv-JunΔDBD.GFP) were distributed much more widely within the syncytium than their wild-type counterparts (Lv-Alx1.WT.mCherry, Lv-Ets1.WT.mCherry and Lv-Jun.WT.mCherry). (d) Deletion of DBDs also caused transcription factors to be less tightly restricted to the cell nucleus, as shown for Lv-Alx1. Top row: GFP fluorescence. Middle row: mCherry fluorescence overlaid onto differential interference contrast (DIC) images. Scale bars: 50 μm. (C) Cell counts. Live embryos were imaged by conventional epifluorescence microscopy. For each embryo, one or two focal planes were collected; these were typically anal views that imaged PMC cell bodies along the postoral and body rods. The numbers of cell bodies within the PMC syncytium that contained the indicated mCherry-tagged, wild-type protein or GFP-tagged mutant protein were counted. Data are mean±s.d. *P*-values were calculated using two-sample paired *t*-tests (*P<0.05). See also Table S2.

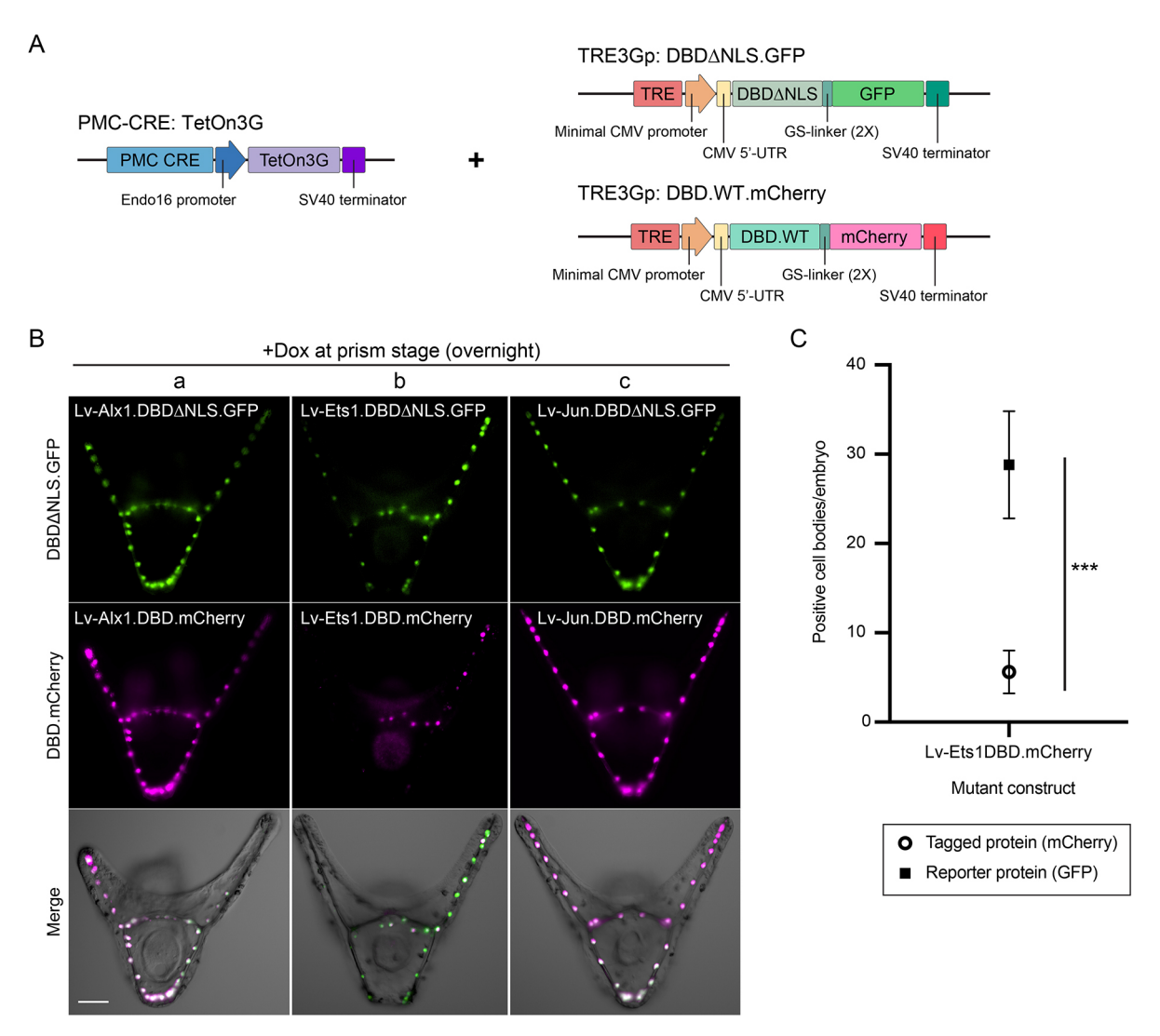


Fig. 5. The DNA-binding domain of Lv-Ets1, but not those of other transcription factors expressed by PMCs, is sufficient to reduce the mobility of mCherry. (A) Schematic representation of the Tet-On transactivator and responder constructs used to induce PMC-specific expression of GFP and mCherry fusion proteins. Each line drawing represents a separate plasmid. (B) Anal views of live transgenic pluteus larvae after Dox-induced gene expression. (a,c) Fusion proteins containing the complete DNA-binding domains (DBDs) (DNA-binding motifs+nuclear localization sequences) of Lv-Alx1 (Lv-Alx1.DBD.mCherry) and Lv-Jun (Lv-Jun.DBD.mCherry) were distributed throughout the PMC syncytium, as were fusion proteins containing DBDs that lacked nuclear localization sequences (Lv-Alx1.DBDΔNLS.GFP and Lv-Jun.DBDΔNLS.GFP). (b) In contrast, fusion of the complete DBD of Lv-Ets1 to mCherry (Lv-Ets1.DBD-mCherry) markedly reduced the mobility of the protein. This effect was dependent, at least in part, on nuclear localization sequences within the DBD, as shown by the increased mobility of Lv-Ets1.DBDΔNLS.GFP. Top row: GFP fluorescence. Middle row: mCherry fluorescence. Bottom row: GFP and mCherry fluorescence overlaid onto differential interference contrast (DIC) images. Scale bar: 50 μm. (C) Cell counts. Live embryos were imaged by conventional epifluorescence microscopy. For each embryo, one or two focal planes were collected; these were typically anal views that imaged PMC cell bodies along the postoral and body rods. The numbers of cell bodies within the PMC syncytium that contained Lv-Ets1DBD.mCherry or a diffusible reference protein (GFP) were counted. Data are mean±s.d. *P*-values were calculated using two-sample paired *t*-tests (****P*<0.001). See also Table S2.

2006; Mann et al., 2010). We hypothesized that secretory activity within the PMC syncytium might be localized, thereby restricting the distribution of such proteins. To test this hypothesis, we examined the distribution of mutant forms of Lv-P16, Lv-SM29 and Lv-Clectin that lacked N-terminal endoplasmic reticulum (ER) signal sequences. Deletion of the signal sequence of Lv-Clectin (Lv-ClectinΔSS.GFP) dramatically expanded the distribution of the protein compared with the wild-type form (Fig. 6Bc,C; Fig. S2D). Deletion of the N-terminal signal sequence of Lv-SM29 also expanded the distribution of the protein within the syncytium, but more modestly (Fig. 6Bd; Fig. S2E). We noted that,

although wild-type Lv-SM29 was localized in prominent puncta that were often observed in filopodia distant from PMC cell bodies (Fig. S1B), the mutant form was localized in PMC cell bodies and was not concentrated in puncta. Consistent with observations made using the constitutive expression system, deletion of the signal sequence of Lv-P16 (Lv-P16ΔSS.GFP) had no detectable effect on the distribution of the protein within the PMC syncytium, although it altered the subcellular localization of the protein, as described above (Fig. 1Be, Fig. 6Ba). P16 also contains a predicted transmembrane domain, which is located near the C terminus of the protein. Deletion of the transmembrane domain alone (Lv-

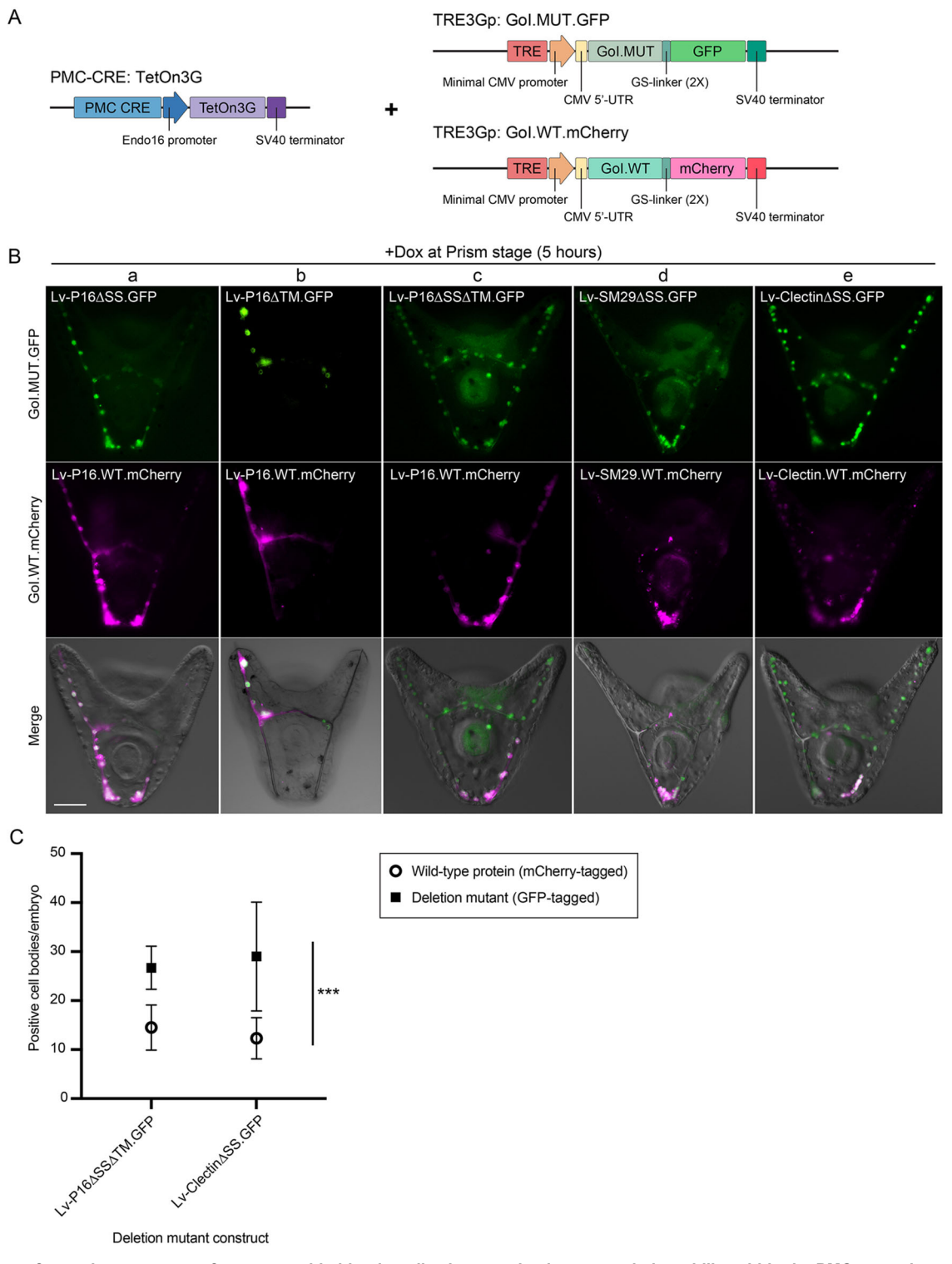


Fig. 6. Deletion of targeting sequences from sea urchin biomineralization proteins increases their mobility within the PMC syncytium.

(A) Schematic representation of the Tet-On transactivator and responder constructs used to induce PMC-specific expression of GFP and mCherry fusion proteins. Each line drawing represents a separate plasmid. (B) Anal views of live transgenic pluteus larvae after Dox-induced gene expression. (a,b) Single deletions of the N-terminal endoplasmic reticulum signal sequence or the C-terminal transmembrane domain of Lv-P16 (Lv-P16ΔSS.GFP and Lv-P16ΔTM.GFP) had little effect on the distribution of the protein. (c) Deletion of both motifs (Lv-P16ΔSSΔTM.GFP) markedly increased mobility. (d,e) Deletion of the signal sequences of Lv-Clectin (Lv-ClectinΔSS.GFP) and Lv-SM29 (Lv-SM29ΔSS.GFP), proteins that lack other targeting motifs, increased mobility relative to the corresponding wild-type forms of these proteins, although this effect was more pronounced in the case of Lv-Clectin. Top row: GFP fluorescence. Middle row: mCherry fluorescence. Bottom row: GFP and mCherry fluorescence overlaid onto differential interference contrast (DIC) images. Gol: gene of interest. Scale bar: 50 μm. (C) Cell counts. Live embryos were imaged by conventional epifluorescence microscopy. For each embryo, one or two focal planes were collected; these were typically anal views that imaged PMC cell bodies along the postoral and body rods. The numbers of cell bodies within the PMC syncytium that contained the indicated mCherry-tagged, wild-type protein or GFP-tagged mutant protein were counted. Data are mean±s.d. P-values were calculated using two-sample paired t-tests (***P<0.001). See also Table S2.

P16 Δ TM.GFP) also had little or no effect on the distribution of the protein (Fig. 6Bb). Deletion of both the N-terminal signal sequence and the transmembrane domain, however, dramatically enhanced the mobility of the protein within the PMC syncytium (Fig. 6Bc,C; Fig. S2F, Table S2). This mutant form of Lv-P16 was localized primarily in the cytoplasm.

To further explore the role of N-terminal signal sequences in regulating the mobility of proteins within the PMC syncytium, we examined the distribution of chimeric forms of GFP that contained the N-terminal signal sequences of Lv-P16, Lv-SM29 or Lv-Clectin (Fig. 7). In all cases, N-terminal signal sequences were inserted immediately downstream of the start codon and were separated from the remainder of the GFP polypeptide by two tandem copies of a flexible, glycine/serine-rich linker. Each of these mutant forms of GFP was detected at only very low levels in the PMC syncytium, distinctly lower than when GFP was expressed alone. This may be because the folding and stability of GFP was altered by addition of the N-terminal signal sequence or because the fusion protein was secreted into the extracellular environment. Others have reported that GFP folding can be perturbed when fusion proteins are targeted to the lumen of the ER (Valbuena et al., 2020). Nevertheless, in embryos with detectable levels of these fusion proteins, the proteins were often restricted to a sub-domain of the PMC syncytium (>50% of embryos in each case), which was never observed with GFP (Fig. 7Ba,d,e). As P16 contains a transmembrane domain in addition to an N-terminal signal sequence, and because our previous studies suggested that the transmembrane domain might influence the mobility of P16 within the syncytium, we also tested the effect of linking the Lv-P16 transmembrane domain to GFP. As in studies with N-terminal signal sequences, the Lv-P16 transmembrane domain was inserted immediately downstream of the start codon and separated from the remainder of the GFP sequence by two tandem copies of a glycine/serine-rich spacer. The chimeric Lv-P16TM.GFP protein exhibited a restricted distribution in 87% of transgenic embryos that expressed the protein (n=23) (Fig. 7Bb, Fig. 7C; Table S2), indicating that the P16 transmembrane sequence was sufficient to limit protein mobility within the PMC syncytium. A form of this protein that also contained the N-terminal signal sequence of Lv-P16 exhibited a similar, highly restricted distribution (Fig. 7Bc).

DISCUSSION

We have used the skeletogenic mesenchyme of the sea urchin embryo as a model for discovering mechanisms that generate specialized molecular and functional domains within syncytia. The distributions of endogenous proteins within the PMC syncytium likely depend on a complex combination of factors, including RNA expression patterns, RNA and protein expression levels, and RNA and protein stability. In this study, we focused on protein mobility and showed that the movement of transcription factors and biomineralization proteins is restricted within the PMC syncytium, providing a mechanism for generating stable compartments of gene expression and restricting the functional domains of effector proteins.

The mobility of proteins within the PMC syncytium is likely regulated by diverse mechanisms. Protein size alone is evidently not a major determinant of mobility, as we have documented several relatively large proteins (MW=66-76 kDa) that are highly mobile, including Lv-Alx1ΔDBD.GFP, Lv-Ets1ΔDBD.GFP (both from this study), Sp-caMEK.GFP and Sp-DUSP6.GFP (Khor and Ettensohn, 2023), as well as much smaller proteins with very limited mobility (e.g. Lv-P16TM.GFP, MW=31.5 kDa). Many of the proteins that regulate biomineralization, including those of the MSP130, P16 and

spicule matrix protein families, are secreted or membrane-associated proteins (Livingston et al., 2006; Mann et al., 2010). The presence of N-terminal, ER signal sequences on these proteins could recruit these proteins co-translationally to nearby ER membranes and thereby locally target secretion. Ultrastructural analysis of the PMC syncytium has shown that Golgi stacks are restricted to the perinuclear regions of PMC cell bodies and are absent from the cytoplasmic cable (Gibbins et al., 1969), suggesting that secretory activity is spatially localized within the syncytium at the level of individual cell bodies. In the present study, we found that N-terminal fusions of the ER signal sequences of biomineralization proteins markedly reduced the mobility of GFP within the syncytium. In addition, deletion of the N-terminal ER signal sequences of biomineralization proteins expanded their distributions within the syncytium, although to varying degrees, and the mobility of one protein (P16) was also regulated by its transmembrane domain. With respect to transcription factors, deletion of DNA-binding domains and their associated nuclear localization sequences demonstrated the importance of these sequences in restricting mobility within the syncytium. Fusions of these sequences to fluorescent reporters, however, indicate that other domains of transcription factors also contribute to their restricted mobility. These might include, for example, motifs that mediate protein-protein interactions.

Endogenous mRNAs are often more tightly localized within the PMC syncytium than are the clonal territories of mRNA expression we typically observed in transgenic embryos. This implies that endogenous proteins can have much more restricted distributions than the patterns of exogenous reporter proteins that we observed. For example, at late embryonic stages, p16 mRNA is restricted to just two or three cells at the tip of each arm (Cheers and Ettensohn, 2005), suggesting that the distribution of this protein may be very tightly restricted at these stages. It should be noted that many (although not all) genes in the skeletogenic GRN are initially expressed by all PMCs and their transcripts are restricted to specific sub-domains of the syncytium later in development. The extent to which initial, broad patterns of protein expression might be replaced by region-specific patterns would depend on protein perdurance. It should be also borne in mind that if molecules of a biomineralization protein such as P16 are not re-used during skeletogenesis, perhaps because they are irreversibly incorporated into the growing biomineral, then only newly synthesized protein will support skeletal growth. In this case, the limited expression and mobility of biomineralization proteins at late stages could dramatically restrict skeletal growth to specific sites, regardless of any earlier, more general pattern of protein expression.

Our study does not address the mechanisms that underlie the localized distributions of mRNAs within the PMC syncytium. The highly localized distribution in transgenic embryos of a wide variety of experimentally expressed mRNAs, which lack any native subcellular targeting motifs, clearly shows that exogenous RNAs have very limited mobility within the PMC syncytium. We strongly favor the view that the same is true of endogenous mRNAs; i.e. that mRNAs remain near the site of synthesis. Formally, however, the possibility cannot be excluded that endogenous mRNAs translocate over long distances and are directionally targeted to (or trapped at) specific sites within the PMC syncytium. However, complex mechanisms would be required to account for the long-distance movements of a large number of endogenous mRNAs and their selective targeting to several diverse locations within the syncytium.

It is noteworthy that, although our study involved the overexpression of a variety of proteins using both constitutive and inducible expression systems, we did not detect major perturbations of skeletal growth or

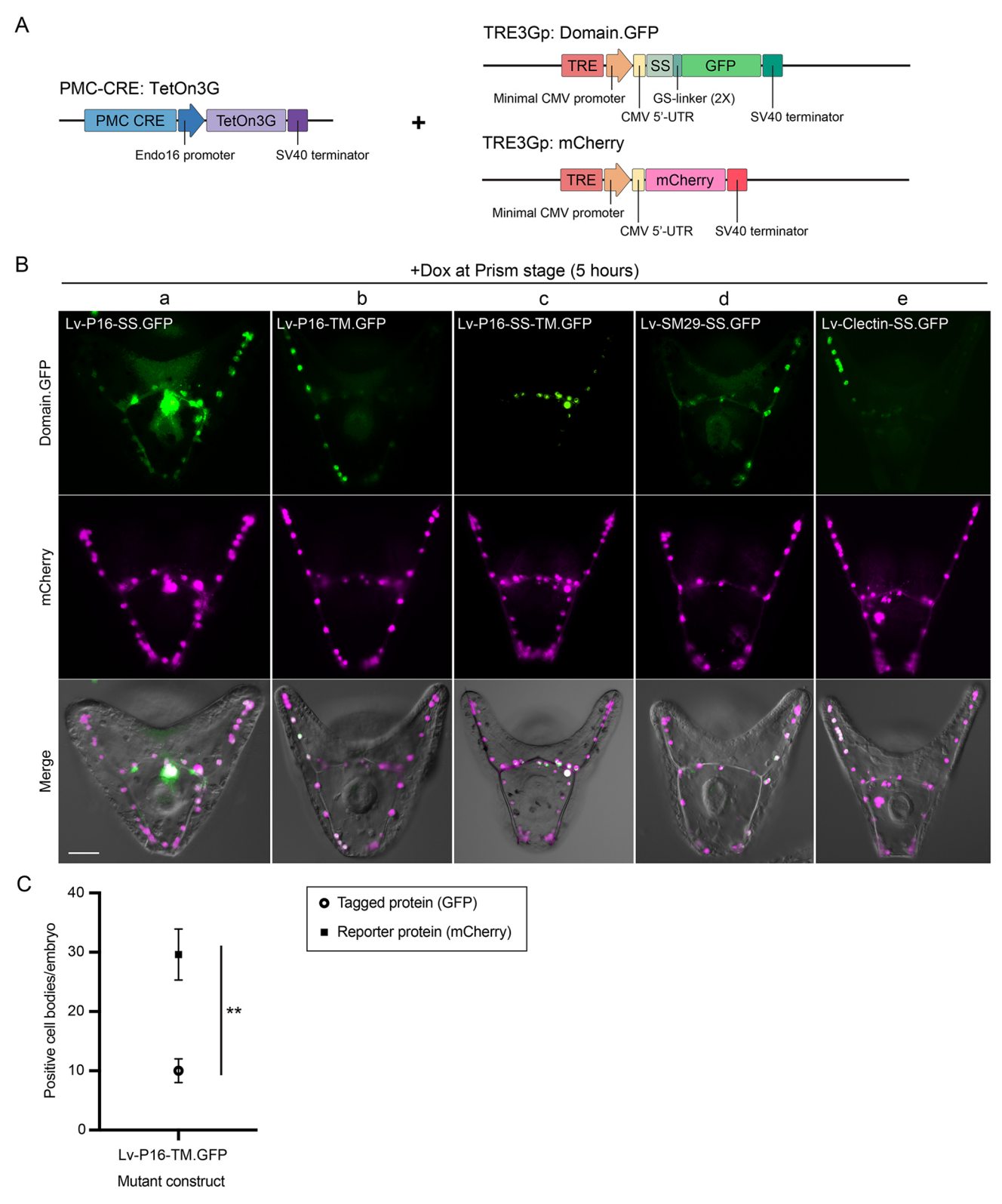


Fig. 7. Fusion of targeting sequences of sea urchin biomineralization proteins to GFP reduces mobility. (A) Schematic representation of the Tet-On transactivator and responder constructs used to induce PMC-specific expression of GFP fusion proteins and wild-type mCherry. Each line drawing represents a separate plasmid. (B) Anal views of live transgenic pluteus larvae after Dox-induced gene expression. N-terminal fusions of the signal sequences of Lv-SM29, Lv-Clectin or Lv-P16 to GFP (Lv-P16-SS.GFP, Lv-SM29-SS.GFP and Lv-Clectin-SS.GFP), or fusion of the transmembrane domain of P16, alone (Lv-P16-TM.GFP) or in combination with the Lv-P16 signal sequence (Lv-P16-SS-TM.GFP) reduced the mobility of the fusion proteins within the PMC syncytium compared with mCherry. Top row: GFP fluorescence. Middle row: mCherry fluorescence. Bottom row: GFP and mCherry fluorescence overlaid onto differential interference contrast (DIC) images. Scale bar: 50 µm. (C) Cell counts. Live embryos were imaged by conventional epifluorescence microscopy. For each embryo, one or two focal planes were collected; these were typically anal views that imaged PMC cell bodies along the postoral and body rods. The numbers of cell bodies within the PMC syncytium that contained Lv-P16-TM.GFP or a diffusible reference protein (mCherry) were counted. Data are mean ±s.d. *P*-values were calculated using two-sample, paired *t*-tests (***P*<0.01). See also Table S2.

patterning, with the exception of the apparent disruption of PMC specification caused by constitutive expression of Lv-Ets1. It is possible, however, that if proteins were expressed at higher levels they would perturb skeletal growth.

Our findings are consistent with a model of skeletal patterning which proposes that local ectoderm-derived cues control the expression or activity of regulatory (i.e. transcription factorencoding) genes in the skeletogenic GRN, creating sub-domains of gene expression within the syncytium that are stable due to the limited mobility of transcription factors (Fig. 8). According to this model, local differences in the regulatory states of PMC nuclei subsequently lead to differences in the expression of downstream effector genes, including those that are regulators of biomineral growth. Given the complex suite of signaling molecules that regulates skeletal growth, there may be diverse signaling environments within the syncytium that generate multiple distinct regulatory states. This could explain the diverse expression patterns of biomineralization genes controlled by the PMC GRN (Sun and Ettensohn, 2014). The limited mobility of biomineralization proteins within the syncytium would be expected to generate sub-domains characterized by distinct constellations of biomineralization proteins, which we propose results in local patterns of skeletal growth. Beyond simply determining whether biomineral is deposited or not in a given sub-domain of the syncytium (as illustrated in the simplified model shown in Fig. 8), local expression patterns of biomineralization proteins might regulate more subtle aspects of skeletal patterning, such as skeletal rod morphology (i.e. simple versus

fenestrated or smooth versus barbed), growth rate, crystallographic axis of growth or sites of branching, all of which are features of growth that are likely regulated by proteins associated with the growing biomineral (Weiner, 2008; Veis, 2011; Marin et al., 2016).

Although this model emphasizes regulation at the transcriptional level, post-translational mechanisms may also contribute to local patterns of skeletal growth. Here, again, the restricted mobility of proteins within the syncytium is likely to play a key role. If ectodermderived cues result in the post-translational modification of PMC transcription factors, the restricted mobility of these proteins within the syncytium (which we observed with all transcription factors tested) would generate sub-domains of activated (or repressed) forms. Considerable evidence supports the view that such a mechanism operates during normal skeletogenesis and accounts for the regulation of skeletal growth by VEGF3. A key transcription factor in the PMC GRN, Ets1, is positively regulated by ERK signaling (Röttinger et al., 2004), a pathway activated by VEGF receptors in many cell types (Cross et al., 2003; Holmes et al., 2007; Claesson-Welsh and Welsh, 2013). Although the pivotal role of Ets1 in the initial, cell-autonomous activation of the skeletogenic GRN is well established, until recently it was unknown whether Ets1 continues to provide regulatory inputs at post-gastrula stages, when the PMC GRN and skeletal growth are regulated by VEGF3. Recent studies using the conditional Tet-On system to perturb Ets1 function and manipulate the expression of positive and negative regulators of the ERK pathway specifically in PMCs have shown that Ets1 and

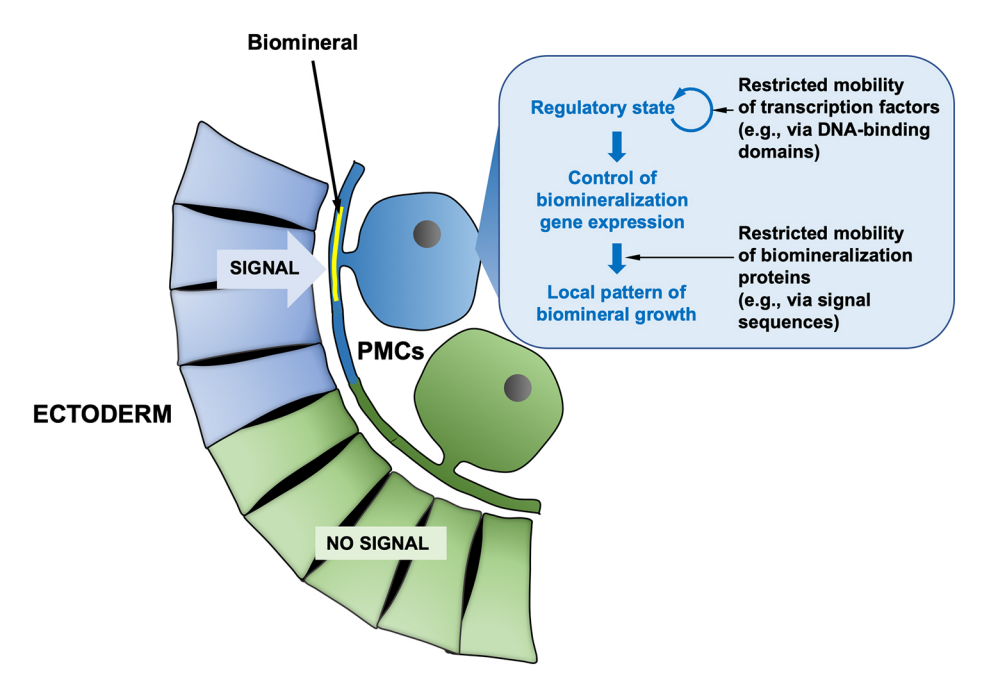


Fig. 8. A model for the local control of skeletal growth in the PMC syncytium. Previous studies have shown that signaling ligands, including VEGF3 (Duloquin et al., 2007), are secreted by specific ectodermal territories and lead to the localized expression of regulatory (transcription factor-encoding) genes in the nuclei of nearby PMC cell bodies (Sun and Ettensohn, 2014; Tarsis et al., 2022). The present study shows that distinct nuclear regulatory states are maintained in sub-domains of the syncytium due to the limited mobility of the transcription factors. We propose that these local regulatory states, in turn, generate territory-specific patterns of expression of effector genes, which are well documented (e.g. Harkey et al., 1992; Guss and Ettensohn, 1997; Illies et al., 2002; Livingston et al., 2006; Sun and Ettensohn, 2014). We hypothesize that such effector genes include key regulators of biomineral growth. The present study and previous work (Wilt et al., 2008) demonstrate that many biomineralization proteins also have limited mobility within the PMC syncytium, creating distinct sub-domains of protein expression. Our model proposes that the localized expression of biomineralization proteins underlies the regional patterns of skeletal growth that have been previously described (Guss and Ettensohn, 2007; Descoteaux et al., 2023). The diagram illustrates only two distinct nuclear regulatory states (blue and green), whereas there may be many diverse regulatory stages within the PMC syncytium. The diagram is also simplified, as it suggests that signaling determines only whether or not biomineral is deposited, whereas we hypothesize that region-specific expression of biomineralization proteins also regulate other aspects of skeletal patterning, such as skeletal rod morphology, growth rate and branching (see Discussion). The model requires that components of signal transduction pathways downstream of VEGF and other ligands have limited mobility within the PMC syncytium, although this is not shown.

ERK signaling continue to regulate skeletogenesis after the formation of the PMC syncytium (Khor and Ettensohn, 2023). The restricted mobility of Ets1, the regulation of its activity by ERK signaling, and the essential late inputs from Ets1 and ERK into skeletogenic genes, make Ets1 an attractive candidate for linking ectodermal signaling to skeletal patterning.

Our findings are relevant to the functional and molecular compartmentalization of other syncytia. Heterogeneous patterns of gene expression have been documented in several other syncytia, including vertebrate muscle (Bursztajn et al., 1989) and syncytiotrophoblast (Fogarty et al., 2011), slime mold pseudoplasmodia (Gerber et al., 2022), and multinucleate fungi (Dundon et al., 2016), although the molecular mechanisms that establish and maintain these domains are not well understood. In the best-studied case, the early syncytial development of *Drosophila* embryos, anterior-posterior compartments of gene expression are generated through the limited diffusibility of several transcription factors, including Bicoid (Huang and Saunders, 2020). The restricted mobility of transcription factors is likely to be a prerequisite for the establishment of gene expression compartments in syncytia. In some instances, such as the skeletogenic syncytium of the sea urchin embryo, the limited mobility of effector proteins encoded by downstream target genes subsequently generates functional compartments within the syncytium.

MATERIALS AND METHODS

Animals

Gravid adult *Lytechinus variegatus* were obtained from Pelagic (Sugarloaf Key, FL, USA). Spawning was induced by intracoelomic injection of 0.5 M KCl. *L. variegatus* embryos were cultured in artificial seawater (ASW) at 18-25°C in temperature-controlled incubators.

DNA constructs

Plasmids used in this study were generated as previously described (Khor and Ettensohn, 2023) with a few modifications. For the transgenic activator construct, the TetOn3G recombinant gene, based on the transactivator sequence from pCAG-TetOn-3G (Faedo et al., 2017), was synthesized as a gBlock gene fragment by Integrated DNA Technologies. The gBlock was cloned into EpGFPII in place of the GFP-coding sequence, downstream of the Sp-endo16 promoter. To drive PMC-specific expression, an intronic cisregulatory element (CRE) of LOC115919257 (a gene previously referred to as WHL22.691495 or *Sp-EMI/TM*, and characterized by Khor et al., 2019) was cloned upstream of the promoter to generate PMC-CRE: TetOn3G. The TRE3Gp promoter containing the Tet response element (TRE), minimal human cytomegalovirus (CMV) promoter and CMV 5'-UTR (Kang et al., 2019) was cloned upstream of the eGFP- or mCherry-coding sequence to generate transgenic responder constructs. Tagged fusion proteins were generated by fusing GFP or mCherry to their C termini with a glycine/ serine-rich linker (GGGGSGGGS).

Doxycycline treatment

A stock solution of 10 mg/ml doxycycline hyclate (Dox) (D9891, Sigma-Aldrich) was prepared using sterile $\rm H_2O$ and stored in light-protected microcentrifuge tubes at $-20^{\circ}\rm C$. Dox was added to the culture medium (sea water) to yield a final concentration of 5 µg/ml. In all experiments, Dox was added at the prism stage, after PMC fusion was complete and the syncytium was well formed. Embryos were typically examined after 5-6 h of Dox exposure, at the early two-armed pluteus stage. In some experiments, embryos were allowed to develop overnight in the presence of the drug and scored at the late two-armed pluteus stage.

Microinjection

Linearized plasmids were injected into fertilized *L. variegatus* eggs by following established protocols (Arnone et al., 2004; Cheers and Ettensohn, 2004). Each 20 µl injection solution contained 50 ng of the transactivator

plasmid, 50 ng of each responder plasmid, 500 ng of HindIII-digested genomic DNA, 0.12 M KCl, 20% glycerol and 0.1% Texas Red-Dextran (10,000 MW). Linear DNA injected into fertilized eggs forms a large concatemer that is randomly inherited by one or a few cells during cleavage (McMahon et al., 1985). Table S1 lists all of the constructs that were injected during the course of this study and indicates the number of biological replicates (separate injections using embryos from different mating pairs). For each replicate, at least 10 embryos that expressed the transgenes were scored.

ImmunoFISH

Combined whole-mount fluorescent *in situ* hybridization and immunofluorescence staining (ImmunoFISH) were carried out as previously described (Khor and Ettensohn, 2023). A DNA template containing the GFP-coding sequence was PCR amplified with a reverse primer that contained a T3 promoter sequence. Digoxigenin-labeled RNA probes were synthesized using the MEGAscript T3 Transcription Kit (Invitrogen/Thermo Fisher Scientific).

Imaging

Images were collected using an Olympus BX60 microscope fitted with a 20× dry objective (N.A., 0.7), an X-Cite XYLIS LED light source (Excelitas Technologies) and a Xyla 4.2 sCMOS camera (Oxford Instruments). Images were processed using cellSens imaging software (Olympus) and Fiji/ImageJ version 2.9.0/1.53t (Schindelin et al., 2012).

Acknowledgements

The authors are grateful to Dr Brooke McCartney for many valuable suggestions regarding the manuscript.

Competing interests

The authors declare no competing or financial interests.

Author contributions

Conceptualization: J.M.K., C.A.E.; Methodology: J.M.K., J.G.-S., C.A.E.; Validation: J.M.K., J.G.-S., C.A.E.; Formal analysis: J.M.K., C.A.E.; Investigation: C.A.E.; Resources: C.A.E.; Writing - original draft: C.A.E.; Writing - review & editing: J.M.K., C.A.E.; Visualization: J.M.K., C.A.E.; Supervision: C.A.E.; Project administration: C.A.E.; Funding acquisition: C.A.E.

Funding

This work was supported by the National Science Foundation (IOS2004952 to C.A.E.).

Data availability

All relevant data can be found within the article and its supplementary information.

The people behind the papers

This article has an associated 'The people behind the papers' interview with some of the authors.

Peer review history

The peer review history is available online at https://journals.biologists.com/dev/lookup/doi/10.1242/dev.201804.reviewer-comments.pdf.

References

Adomako-Ankomah, A. and Ettensohn, C. A. (2013). Growth factor-mediated mesodermal cell guidance and skeletogenesis during sea urchin gastrulation. *Development* 140, 4214-4225. doi:10.1242/dev.100479

Adomako-Ankomah, A. and Ettensohn, C. A. (2014). Growth factors and early mesoderm morphogenesis: insights from the sea urchin embryo. *Genesis* 52, 158-172. doi:10.1002/dvg.22746

Amore, G. and Davidson, E. H. (2006). cis-Regulatory control of cyclophilin, a member of the ETS-DRI skeletogenic gene battery in the sea urchin embryo. *Dev. Biol.* 293, 555-564. doi:10.1016/j.ydbio.2006.02.024

Armstrong, N., Hardin, J. and Mcclay, D. R. (1993). Cell-cell interactions regulate skeleton formation in the sea urchin embryo. *Development* 119, 833-840. doi:10. 1242/dev.119.3.833

Arnone, M. I., Bogarad, L. D., Collazo, A., Kirchhamer, C. V., Cameron, R. A., Rast, J. P., Gregorians, A. and Davidson, E. H. (1997). Green Fluorescent Protein in the sea urchin: new experimental approaches to transcriptional

- regulatory analysis in embryos and larvae. *Development* **124**, 4649-4659. doi:10. 1242/dev 124 22 4649
- Arnone, M. I., Dmochowski, I. J. and Gache, C. (2004). Using reporter genes to study cis-regulatory elements. *Methods Cell Biol.* 74, 621-652. doi:10.1016/ S0091-679X(04)74025-X
- Arshinoff, B. I., Cary, G. A., Karimi, K., Foley, S., Agalakov, S., Delgado, F., Lotay, V. S., Ku, C. J., Pells, T. J., Beatman, T. R. et al. (2022). Echinobase: leveraging an extant model organism database to build a knowledgebase supporting research on the genomics and biology of echinoderms. *Nucleic Acids Res.* 50, D970-D979. doi:10.1093/nar/gkab1005
- Ben-Tabou De-Leon, S. (2022). The evolution of biomineralization through the cooption of organic scaffold forming networks. *Cells* 11, 595. doi:10.3390/cells11040595
- Boulukos, K. E., Pognonec, P., Rabault, B., Begue, A. and Ghysdael, J. (1989). Definition of an Ets1 protein domain required for nuclear localization in cells and DNA-binding activity in vitro. *Mol. Cell. Biol.* **9**, 5718-5721.
- Bursztajn, S., Berman, S. A. and Gilbert, W. (1989). Differential expression of acetylcholine receptor mRNA in nuclei of cultured muscle cells. *Proc. Natl. Acad.* Sci. USA 86, 2928-2932. doi:10.1073/pnas.86.8.2928
- Bzdyl, N. M., Moran, C. L., Bendo, J. and Sarkar-Tyson, M. (2022). Pathogenicity and virulence of Burkholderia pseudomallei. Virulence 13, 1945-1965. doi:10. 1080/21505594.2022.2139063
- Carvalho, L. and Heisenberg, C.-P. (2010). The yolk syncytial layer in early zebrafish development. Trends Cell Biol. 20, 586-592. doi:10.1016/j.tcb.2010.06. 009
- Cheers, M. S. and Ettensohn, C. A. (2004). Rapid microinjection of fertilized eggs. Methods Cell Biol. 74, 287-310. doi:10.1016/S0091-679X(04)74013-3
- Cheers, M. S. and Ettensohn, C. A. (2005). P16 is an essential regulator of skeletogenesis in the sea urchin embryo. *Dev. Biol.* 283, 384-396. doi:10.1016/j. ydbio.2005.02.037
- Claesson-Welsh, L. and Welsh, M. (2013). VEGFA and tumour angiogenesis. J. Intern. Med. 273, 114-127. doi:10.1111/joim.12019
- Cross, M. J., Dixelius, J., Matsumoto, T. and Claesson-Welsh, L. (2003). VEGF-receptor signal transduction. *Trends Biochem. Sci.* **28**, 488-494. doi:10.1016/S0968-0004(03)00193-2
- Damle, S. and Davidson, E. H. (2011). Precise cis-regulatory control of spatial and temporal expression of the alx-1 gene in the skeletogenic lineage of s. purpuratus. *Dev. Biol.* 357, 505-517. doi:10.1016/j.ydbio.2011.06.016
- Davidson, P. L., Guo, H., Wang, L., Berrio, A., Zhang, H., Chang, Y., Soborowski, A. L., Mcclay, D. R., Fan, G. and Wray, G. A. (2020). Chromosomal-level genome assembly of the sea urchin *Lytechinus variegatus* substantially improves functional genomic analyses. *Genome Biol. Evol.* 12, 1080-1086. doi:10.1093/gbe/evaa101
- Descoteaux, A. E., Zuch, D. T. and Bradham, C. A. (2023). Polychrome labeling reveals skeletal triradiate and elongation dynamics and abnormalities in patterning cue-perturbed embryos. *Dev. Biol.* 498, 1-13. doi:10.1016/j.ydbio. 2023.03.003
- **Duboc, V., Röttinger, E., Besnardeau, L. and Lepage, T.** (2004). Nodal and BMP2/4 signaling organizes the oral-aboral axis of the sea urchin embryo. *Dev. Cell* **6**, 397-410. doi:10.1016/S1534-5807(04)00056-5
- Duloquin, L., Lhomond, G. and Gache, C. (2007). Localized VEGF signaling from ectoderm to mesenchyme cells controls morphogenesis of the sea urchin embryo skeleton. *Development* 134, 2293-2302. doi:10.1242/dev.005108
- Dundon, S. E., Chang, S. S., Kumar, A., Occhipinti, P., Shroff, H., Roper, M. and Gladfelter, A. S. (2016). Clustered nuclei maintain autonomy and nucleocytoplasmic ratio control in a syncytium. *Mol. Biol. Cell* 27, 2000-2007. doi:10.1091/mbc.E16-02-0129
- **Ettensohn, C. A.** (2009). Lessons from a gene regulatory network: echinoderm skeletogenesis provides insights into evolution, plasticity and morphogenesis. *Development* **136**, 11-21. doi:10.1242/dev.023564
- Ettensohn, C. A. (2020). The gene regulatory control of sea urchin gastrulation. *Mech. Dev.* **162**, 103599. doi:10.1016/j.mod.2020.103599
- Ettensohn, C. A. and Adomako-Ankomah, A. (2019). The evolution of a new cell type was associated with competition for a signaling ligand. *PLoS Biol.* 17, e3000460. doi:10.1371/journal.pbio.3000460
- Ettensohn, C. A., Guerrero-Santoro, J. and Khor, J. M. (2022). Lessons from a transcription factor: Alx1 provides insights into gene regulatory networks, cellular reprogramming, and cell type evolution. *Curr. Top. Dev. Biol.* **146**, 113-148. doi:10.1016/bs.ctdb.2021.10.005
- Faedo, A., Laporta, A., Segnali, A., Galimberti, M., Besusso, D., Cesana, E., Belloli, S., Moresco, R. M., Tropiano, M., Fucà, E. et al. (2017). Differentiation of human telencephalic progenitor cells into MSNs by inducible expression of Gsx2 and Ebf1. Proc. Natl. Acad. Sci. U.S.A. 114, E1234-E1242. doi:10.1073/pnas. 1611473114
- Flowers, V. L., Courteau, G. R., Poustka, A. J., Weng, W. and Venuti, J. M. (2004). Nodal/activin signaling establishes oral-aboral polarity in the early sea urchin embryo. *Dev. Dyn.* **231**, 727-740. doi:10.1002/dvdy.20194
- Fogarty, N. M., Mayhew, T. M., Ferguson-Smith, A. C. and Burton, G. J. (2011). A quantitative analysis of transcriptionally active syncytiotrophoblast nuclei across human gestation. *J. Anat.* **219**, 601-610. doi:10.1111/j.1469-7580.2011.01417.x

- Fujita, K., Takechi, E., Sakamoto, N., Sumiyoshi, N., Izumi, S., Miyamoto, T., Matsuura, S., Tsurugaya, T., Akasaka, K. and Yamamoto, T. (2010). HpSulf, a heparan sulfate 6-O-endosulfatase, is involved in the regulation of VEGF signaling during sea urchin development. *Mech. Dev.* 127, 235-245. doi:10.1016/j.mod. 2009.12.001
- Gerber, T., Loureiro, C., Schramma, N., Chen, S., Jain, A., Weber, A., Weigert, A., Santel, M., Alim, K., Treutlein, B. et al. (2022). Spatial transcriptomic and single-nucleus analysis reveals heterogeneity in a gigantic single-celled syncytium. *Elife* 11, e69745. doi:10.7554/eLife.69745
- Gibbins, J. R., Tilney, L. G. and Porter, K. R. (1969). Microtubules in the formation and development of the primary mesenchyme in Arbacia punctulata. I. The distribution of microtubules. J. Cell Biol. 41, 201-226. doi:10.1083/jcb.41.1.201
- Gildor, T., Winter, M. R., Layous, M., Hijaze, E. and Ben-Tabou De-Leon, S. (2021). The biological regulation of sea urchin larval skeletogenesis From genes to biomineralized tissue. *J. Struct. Biol.* **213**, 107797. doi:10.1016/j.jsb.2021. 107797
- Gross, J. M., Peterson, R. E., Wu, S.-Y. and Mcclay, D. R. (2003). LvTbx2/3: a T-box family transcription factor involved in formation of the oral/aboral axis of the sea urchin embryo. *Development* 130, 1989-1999. doi:10.1242/dev.00409
- Guss, K. A. and Ettensohn, C. A. (1997). Skeletal morphogenesis in the sea urchin embryo: regulation of primary mesenchyme gene expression and skeletal rod growth by ectoderm-derived cues. *Development* 124, 1899-1908. doi:10.1242/ dev.124.10.1899.
- Harkey, M. A., Whiteley, H. R. and Whiteley, A. H. (1992). Differential expression of the msp130 gene among skeletal lineage cells in the sea urchin embryo: a three dimensional in situ hybridization analysis. *Mech. Dev.* 37, 173-184. doi:10.1016/ 0925-4773(92)90079-Y
- Holmes, K., Roberts, O. L., Thomas, A. M. and Cross, M. J. (2007). Vascular endothelial growth factor receptor-2: structure, function, intracellular signalling and therapeutic inhibition. *Cell. Signal.* 19, 2003-2012. doi:10.1016/j.cellsig.2007. 05.013
- Huang, A. and Saunders, T. E. (2020). A matter of time: Formation and interpretation of the Bicoid morphogen gradient. *Curr. Top. Dev. Biol.* 137, 79-117. doi:10.1016/bs.ctdb.2019.11.016
- Illies, M. R., Peeler, M. T., Dechtiaruk, A. M. and Ettensohn, C. A. (2002). Identification and developmental expression of new biomineralization proteins in the sea urchin Strongylocentrotus purpuratus. *Dev. Genes Evol.* **212**, 419-431. doi:10.1007/s00427-002-0261-0
- Kang, K., Huang, L., Li, Q., Liao, X., Dang, Q., Yang, Y., Luo, J., Zeng, Y., Li, L. and Gou, D. (2019). An improved Tet-on system in microRNA overexpression and CRISPR/Cas9-mediated gene editing. *J. Anim. Sci. Biotechnol.* 10, 43. doi:10. 1186/s40104-019-0354-5
- **Khor, J. M. and Ettensohn, C. A.** (2017). Functional divergence of paralogous transcription factors supported the evolution of biomineralization in echinoderms. *Elife* **6**, e32728. doi:10.7554/eLife.32728
- Khor, J. M. and Ettensohn, C. A. (2023). An optimized Tet-On system for conditional control of gene expression in sea urchins. *Development* 150, dev201373. doi:10.1242/dev.201373
- Khor, J. M., Guerrero-Santoro, J. and Ettensohn, C. A. (2019). Genome-wide identification of binding sites and gene targets of Alx1, a pivotal regulator of echinoderm skeletogenesis. *Development* 146, dev180653. doi:10.1242/dev. 180653
- Kim, J. H., Jin, P., Duan, R. and Chen, E. H. (2015). Mechanisms of myoblast fusion during muscle development. *Curr. Opin. Genet. Dev.* 32, 162-170. doi:10. 1016/j.gde.2015.03.006
- Kloc, M., Subuddhi, A., Uosef, A., Kubiak, J. Z. and Ghobrial, R. M. (2022). Monocyte-macrophage lineage cell fusion. *Int. J. Mol. Sci.* 23, 6553. doi:10.3390/ijms23126553
- Knapp, R. T., Wu, C.-H., Mobilia, K. C. and Joester, D. (2012). Recombinant sea urchin vascular endothelial growth factor directs single-crystal growth and branching in vitro. J. Am. Chem. Soc. 134, 17908-17911. doi:10.1021/ ja309024b
- Koga, H., Morino, Y. and Wada, H. (2014). The echinoderm larval skeleton as a possible model system for experimental evolutionary biology. *Genesis* 52, 186-192. doi:10.1002/dvg.22758
- Leroy, H., Han, M., Woottum, M., Bracq, L., Bouchet, J., Xie, M. and Benichou, S. (2020). Virus-mediated cell-cell fusion. *Int. J. Mol. Sci.* 21, 9644. doi:10.3390/ijms21249644
- Lin, L., Li, Q., Wang, Y. and Shi, Y. (2021). Syncytia formation during SARS-CoV-2 lung infection: a disastrous unity to eliminate lymphocytes. *Cell Death Differ.* 28, 2019-2021. doi:10.1038/s41418-021-00795-y
- Livingston, B. T., Killian, C. E., Wilt, F., Cameron, A., Landrum, M. J., Ermolaeva, O., Sapojnikov, V., Maglott, D. R., Buchanan, A. M. and Ettensohn, C. A. (2006). A genome-wide analysis of biomineralization-related proteins in the sea urchin Strongylocentrotus purpuratus. *Dev. Biol.* 300, 335-348. doi:10.1016/j.ydbio.2006.07.047
- **Luo, Y.-J. and Su, Y.-H.** (2012). Opposing nodal and BMP signals regulate left-right asymmetry in the sea urchin larva. *PLoS Biol.* **10**, e1001402. doi:10.1371/journal. pbio.1001402

- Mann, K., Wilt, F. H. and Poustka, A. J. (2010). Proteomic analysis of sea urchin (Strongylocentrotus purpuratus) spicule matrix. *Proteome Sci.* 8, 33. doi:10.1186/ 1477-5956-8-33
- Marin, F., Bundeleva, I., Takeuchi, T., Immel, F. and Medakovic, D. (2016). Organic matrices in metazoan calcium carbonate skeletons: Composition, functions, evolution. *J. Struct. Biol.* **196**, 98-106. doi:10.1016/j.jsb.2016.04.006
- Mccartney, B. M. and Dudin, O. (2023). Cellularization across eukaryotes: Conserved mechanisms and novel strategies. Curr. Opin. Cell Biol. 80, 102157. doi:10.1016/j.ceb.2023.102157
- Mcclay, D. R. (2016). Sea urchin morphogenesis. Curr. Top. Dev. Biol. 117, 15-29. doi:10.1016/bs.ctdb.2015.11.003
- Mcintyre, D. C., Seay, N. W., Croce, J. C. and Mcclay, D. R. (2013). Short-range Wnt5 signaling initiates specification of sea urchin posterior ectoderm. Development 140, 4881-4889. doi:10.1242/dev.095844
- Mcintyre, D. C., Lyons, D. C., Martik, M. and Mcclay, D. R. (2014). Branching out: origins of the sea urchin larval skeleton in development and evolution. *Genesis* 52, 173-185. doi:10.1002/dvg.22756
- Mcmahon, A. P., Flytzanis, C. N., Hough-Evans, B. R., Katula, K. S., Britten, R. J. and Davidson, E. H. (1985). Introduction of cloned DNA into sea urchin egg cytoplasm: replication and persistence during embryogenesis. *Dev. Biol.* 108, 420-430. doi:10.1016/0012-1606(85)90045-4
- Mela, A. P., Rico-Ramírez, A. M. and Glass, N. L. (2020). Syncytia in Fungi. Cells 9, 2255. doi:10.3390/cells9102255
- Morgulis, M., Gildor, T., Roopin, M., Sher, N., Malik, A., Lalzar, M., Dines, M., Ben-Tabou De-Leon, S., Khalaily, L. and Ben-Tabou De-Leon, S. (2019). Possible cooption of a VEGF-driven tubulogenesis program for biomineralization in echinoderms. *Proc. Natl. Acad. Sci. USA* **116**, 12353-12362. doi:10.1073/pnas. 1902126116
- Morgulis, M., Winter, M. R., Shternhell, L., Gildor, T. and Ben-Tabou De-Leon, S. (2021). VEGF signaling activates the matrix metalloproteinases, MmpL7 and MmpL5 at the sites of active skeletal growth and MmpL7 regulates skeletal elongation. Dev. Biol. 473, 80-89. doi:10.1016/j.ydbio.2021.01.013
- Morino, Y., Koga, H., Tachibana, K., Shoguchi, E., Kiyomoto, M. and Wada, H. (2012). Heterochronic activation of VEGF signaling and the evolution of the skeleton in echinoderm pluteus larvae. *Evol. Dev.* 14, 428-436. doi:10.1111/j. 1525-142X.2012.00563.x
- Ogle, B. M., Cascalho, M. and Platt, J. L. (2005). Biological implications of cell fusion. Nat. Rev. Mol. Cell Biol. 6, 567-575. doi:10.1038/nrm1678
- Okamura, K., Yamashita, S., Ando, H., Horibata, Y., Aoyama, C., Takagishi, K., Izumi, T., Vance, D. E. and Sugimoto, H. (2009). Identification of nuclear localization and nuclear export signals in Ets2, and the transcriptional regulation of Ets2 and CTP:phosphocholine cytidylyltransferase alpha in tetradecanoyl-13-acetate or macrophage-colony stimulating factor stimulated RAW264 cells. *Biochim. Biophys. Acta* 1791, 173-182. doi:10.1016/j.bbalip.2008.12.016
- Okazaki, K. (1975). Spicule formation by isolated micromeres. *Amer. Zool.* **15**, 567-581. doi:10.1093/icb/15.3.567
- Oliveri, P., Tu, Q. and Davidson, E. H. (2008). Global regulatory logic for specification of an embryonic cell lineage. *Proc. Natl. Acad. Sci. USA* 105, 5955-5962. doi:10.1073/pnas.0711220105
- Olsen, O.-A. (2020). The modular control of cereal endosperm development. *Trends Plant Sci.* 25, 279-290. doi:10.1016/j.tplants.2019.12.003
- Peterson, R. E. and McClay, D. R. (2003). Primary mesenchyme cell patterning during the early stages following ingression. *Dev. Biol.* 254, 68-78
- Rafiq, K., Cheers, M. S. and Ettensohn, C. A. (2012). The genomic regulatory control of skeletal morphogenesis in the sea urchin. *Development* 139, 579-590. doi:10.1242/dev.073049
- Rafiq, K., Shashikant, T., Mcmanus, C. J. and Ettensohn, C. A. (2014). Genome-wide analysis of the skeletogenic gene regulatory network of sea urchins. Development 141, 950-961. doi:10.1242/dev.105585
- Renaud, S. J. and Jeyarajah, M. J. (2022). How trophoblasts fuse: an in-depth look into placental syncytiotrophoblast formation. *Cell. Mol. Life Sci.* **79**, 433. doi:10. 1007/s00018-022-04475-z

- Roberts, S. E. and Gladfelter, A. S. (2015). Nuclear autonomy in multinucleate fundi. *Curr. Opin. Microbiol.* **28**, 60-65. doi:10.1016/ji.mib.2015.08.009
- Röttinger, E., Besnardeau, L. and Lepage, T. (2004). A Raf/MEK/ERK signaling pathway is required for development of the sea urchin embryo micromere lineage through phosphorylation of the transcription factor Ets. *Development* 131, 1075-1087. doi:10.1242/dev.01000 Erratum in: Development 131, 2233.
- Röttinger, E., Saudemont, A., Duboc, V., Besnardeau, L., Mcclay, D. and Lepage, T. (2008). FGF signals guide migration of mesenchymal cells, control skeletal morphogenesis [corrected] and regulate gastrulation during sea urchin development. *Development* 135, 353-365. doi:10.1242/dev.014282
- Schindelin, J., Arganda-Carreras, I., Frise, E., Kaynig, V., Longair, M., Pietzsch, T., Reuden, C., Saalfeld, S., Schmid, B., Tinevez, J. Y. et al. (2012). Fiji: an open-source platform for biological-image analysis. *Nat. Methods* **9**, 676-682. doi:10.1038/nmeth.2019
- Shashikant, T., Khor, J. M. and Ettensohn, C. A. (2018a). Global analysis of primary mesenchyme cell cis-regulatory modules by chromatin accessibility profiling. *BMC Genomics* 19, 206. doi:10.1186/s12864-018-4542-z
- Shashikant, T., Khor, J. M. and Ettensohn, C. A. (2018b). From genome to anatomy: The architecture and evolution of the skeletogenic gene regulatory network of sea urchins and other echinoderms. *Genesis* 56, e23253. doi:10.1002/ dvg.23253
- Stathopoulos, A. and Newcomb, S. (2020). Setting up for gastrulation: D. melanogaster. Curr. Top. Dev. Biol. 136, 3-32. doi:10.1016/bs.ctdb.2019.11. 004
- Sun, Z. and Ettensohn, C. A. (2014). Signal-dependent regulation of the sea urchin skeletogenic gene regulatory network. *Gene Expr. Patterns* **16**, 93-103. doi:10. 1016/j.gep.2014.10.002
- Sun, Z. and Ettensohn, C. A. (2017). TGF-β sensu stricto signaling regulates skeletal morphogenesis in the sea urchin embryo. Dev. Biol. 421, 149-160. doi:10. 1016/j.ydbio.2016.12.007
- Tagawa, T., Kuroki, T., Vogt, P. K. and Chida, K. (1995). The cell cycle-dependent nuclear import of v-Jun is regulated by phosphorylation of a serine adjacent to the nuclear localization signal. J. Cell Biol. 130, 255-263. doi:10.1083/jcb.130.2.255
- Tarsis, K., Gildor, T., Morgulis, M. and Ben-Tabou De-Leon, S. (2022). Distinct regulatory states control the elongation of individual skeletal rods in the sea urchin embryo. Dev. Dyn. 251, 1322-1339. doi:10.1002/dvdy.474
- Urry, L. A., Hamilton, P. C., Killian, C. E. and Wilt, F. H. (2000). Expression of spicule matrix proteins in the sea urchin embryo during normal and experimentally altered spiculogenesis. *Dev. Biol.* 225, 201-213. doi:10.1006/dbio.2000.9828
- Valbuena, F. M., Fitzgerald, I., Strack, R. L., Andruska, N., Smith, L. and Glick, B. S. (2020). A photostable monomeric superfolder green fluorescent protein. *Traffic* 21, 534-544. doi:10.1111/tra.12737
- Veis, A. (2011). Organic matrix-related mineralization of sea urchin spicules, spines, test and teeth. Front. Biosci. (Landmark Ed) 16, 2540-2560. doi:10.2741/3871
- Wahl, M. E., Hahn, J., Gora, K., Davidson, E. H. and Oliveri, P. (2009). The cisregulatory system of the tbrain gene: Alternative use of multiple modules to promote skeletogenic expression in the sea urchin embryo. *Dev. Biol.* 335, 428-441. doi:10.1016/j.ydbio.2009.08.005
- Wang, L., Koppitch, K., Cutting, A., Dong, P., Kudtarkar, P., Zeng, J., Cameron, R. A. and Davidson, E. H. (2019). Developmental effector gene regulation: Multiplexed strategies for functional analysis. *Dev. Biol.* 445, 68-79. doi:10.1016/j. vdbio.2018.10.018
- Weiner, S. (2008). Biomineralization: a structural perspective. J. Struct. Biol. 163, 229-234. doi:10.1016/j.jsb.2008.02.001
- Wilt, F. H., Killian, C. E., Hamilton, P. and Croker, L. (2008). The dynamics of secretion during sea urchin embryonic skeleton formation. *Exp. Cell Res.* 314, 1744-1752. doi:10.1016/j.yexcr.2008.01.036
- Wilt, F., Killian, C. E., Croker, L. and Hamilton, P. (2013). SM30 protein function during sea urchin larval spicule formation. *J. Struct. Biol.* **183**, 199-204. doi:10. 1016/j.jsb.2013.04.001
- Yaguchi, S., Yaguchi, J., Angerer, R. C., Angerer, L. M. and Burke, R. D. (2010). TGFβ signaling positions the ciliary band and patterns neurons in the sea urchin embryo. *Dev. Biol.* **347**, 71-81. doi:10.1016/j.ydbio.2010.08.009